Single gamma-photon revival from sandwich absorbers

R. N. Shakhmuratov, F. Vagizov, and O. Kocharovskaya

Phys. Rev. A **87**, 013807 — Published 7 January 2013

DOI: 10.1103/PhysRevA.87.013807

Single gamma-photon revival from sandwich absorbers

R. N. Shakhmuratov,[1,2] F. Vagizov,[2,3] and O. Kocharovskaya[3]

[1]*Kazan Physical-Technical Institute, Russian Academy of Sciences, 10/7 Sibirsky Trakt, Kazan 420029 Russia*

[2]*Kazan Federal University, 18 Kremlyovskaya Street, Kazan 420008 Russia*

[3]*Department of Physics and Institute for Quantum Studies, TAMU, College Station, Texas 77843-4242, USA*

(Dated: November 9, 2012)

Abstract

The pulsed radiation field propagating in a thick resonant absorber induces the polarization (quantified by the induced atomic dipoles in optical domain or the induced nuclear transition moments in gamma domain), which is distributed oscillatory along the absorber forming a sandwich of polarization layers with opposite phases. As a result, the re-emitted, scattered fields in different layers interfere with the incident input field destructively or constructively, giving rise to the well-known dynamical beats of the output radiation. We propose a method how to force these layers in the sandwich to re-emit in phase with the incident field, which results in a strong radiation burst of short duration at the output of the absorber. We demonstrate this method experimentally for the 14.4 keV nuclear transition in ^{57}Fe.

PACS numbers: 42.50.Gy, 33.45.+x, 76.80.+y

I. INTRODUCTION

Resonant interaction of a single photon with macroscopic absorbers containing atoms, molecules, impurity ions, nuclei, etc. is a cornerstone of quantum mechanics [1]. This is a basic element in coherent (elastic) as well as incoherent (inelastic) interaction of the electromagnetic radiation field with matter employed in modern technology, including telecommunication and optical imaging. Moreover, many proposals how to use single photons and atomic ensembles in quantum communication, quantum memory and computing were discussed recently (for a review, see [2] and references therein). However, there are only a few experiments with single photons and atomic ensembles, and they are usually implemented using either high finesse cavities or auxiliary excitation of atoms by a strong laser fields (see, for example, Ref. [3]). Meanwhile, quantum computations suppose to use large number of qubits and require that each qubit processing must consume only an extremely small amount of energy. Thus, it is preferable to minimize or even avoid any coherent preparation of atomic ensembles by laser pulses.

In this paper we propose and report experimental implementation of a new method of single photon processing (revival and shaping) without initial preparation of a macroscopic absorber. Our method does not require neither cavities no auxiliary coherent fields. We found that the polarization, created in a resonant two-level absorber by a single-photon radiation field, is distributed oscillatory along the absorber forming a sandwich of polarization layers with opposite phases. This leads to either destructive or constructive interference of the re-emitted (scattered) fields from different layers with the incident field, resulting in the well-known dynamical beats of the output radiation. We suggest to divide physically the absorber into slices (two, three or even more) such that at a particular moment of time the phase of the polarization is homogeneous in each slice, i.e., the absorber is divided according to the distribution of the polarization layers at a particular moment of time. If at that time one makes a fast displacement of the odd slices (polarization layers) by a half wavelength of the radiation field ($\lambda/2$) then the phase of the polarization of each slice becomes the same and the radiation fields, scattered by each slice, become in phase with the incident field. Such a polarization phasing produces a short and strong radiation burst at the output of the sliced absorber, which we name the sandwich absorber. This method is especially attractive in gamma domain where high finesse cavities and sources of sufficiently strong co-

herent fields are not available. We make a proof of principal demonstration of the suggested technique in gamma domain with the help of the sandwich absorber whose slices (layers) can be moved rapidly.

We use a weak natural source of gamma-quanta whose energy, 14.4 keV, is resonant to ^{57}Fe nuclei, incorporated randomly into a solid absorber. Each event of 14.4 keV photon emission is heralded by the first photon (122 keV) in a cascade decay of the radioactive ^{57}Co, located in the source. By the time-delayed coincident measurements (TDCM) of two photons (122 keV and 14.4 keV) it is easy to reconstruct the envelope of the single-photon wave-packet (14.4 keV) and to find the change of this envelope after passing through a thick resonant absorber (see, for example, Refs. [4–8] for details). Gamma domain is very convenient for the test experiments with single photons since (i) the detectors have high efficiency in this domain with extremely low level of dark counts, (ii) it is easy to avoid the detection of 14.4 keV photon in the heralded (122 keV) channel by shielding the first detector, for example, with a thin copper foil, and (iii) the 14.4 keV excited state of ^{57}Fe nuclei in the absorber has long lifetime (141 ns) and 14.4 keV photons, emitted by the source, have long coherence time (282 ns) because the emission line of ^{57}Co is predominantly naturally broadened. The last point allows to use simple electronics in a data-acquisition system.

The paper is organized as follows. In Sec. II we present the general formalism of the description of a photon propagation in a thick absorber with a single resonance. In Sec. III we consider the influence of the instantaneous displacement of the absorber on the output radiation field. In Secs. IV, V, and VI we consider the propagation of a single photon through the sandwiches of two and three samples and analyze the effect of a sudden displacement of a separate sample or samples in the sandwich absorbers on the output radiation field. In Sections VII and VIII, the experimental results and their discussion are presented.

II. PHOTON PROPAGATION IN ABSORBING MEDIUM

In this section we outline the method, which we use for the description of a single photon interaction with a dense absorptive medium. As it is shown in Refs. [7, 9], the propagation of a single photon through a macroscopic absorber can be described in the semiclassical approach. Namely, a photon, emitted by the source, is described as a classical pulsed field,

$a_0(z,t)E$, where $a_0(z,t)$ is the photon probability amplitude

$$a_0(z,t) = \Theta\left(t - t_0\right) e^{-(i\omega+\gamma)(t-t_0)+ikz}. \tag{1}$$

Here ω and k are the frequency and wave number of the photon, z is a distance from the source, $2\gamma = \Gamma$ is the decay rate of the excited state, $\Theta(t)$ is the Heaviside step function, and t_0 is the moment of time when the excited state of the source is formed.

Since the amplitude of the single-photon field is very small, its interaction with resonant particles in the absorber is described in the linear response approximation. Namely, the nondiagonal element of the density matrix of each particle, $\rho_{eg} = \sigma_{eg}\exp(-i\omega t + ikz)$, is evolving in accord with the master equation for its slowly varying amplitude σ_{eg},

$$\dot{\sigma}_{eg} = -\gamma\sigma_{eg} + i\Omega(z,t), \tag{2}$$

where $\Omega(z,t) = d_{eg}E_0(z,t)/2\hbar$, d_{eg} is a matrix element of the dipole transition between ground, g, and excited, e, states of a particle, and $E_0(z,t) = a(z,t)E\exp(i\omega t - ikz)$ is a slowly varying field amplitude whose input value at the front face of the absorber is specified by $a_0(z,t)$. Here, for simplicity, the decay rate, γ, of the matter coherence, σ_{eg}, is taken to be the same as the decay rate of the photon probability amplitude and we limit our consideration to the case of exact resonance. Below we adopt the notations conventional in quantum optics and electrodynamics of continuous media (see Ref. [10] for the translation to the notations conventional in gamma-optics).

Slowly varying amplitude of the macroscopic polarization, excited in the medium by the radiation field, is defined by the relation $p(z,t) = Nd_{eg}\sigma_{eg}(z,t)$, where N is the density number of the resonant particles.

In the slowly varying amplitude approximation the 1D wave equation for the radiation field is reduced to

$$\widehat{L}\Omega(z,t) = i\alpha\gamma\sigma_{eg}(z,t)/2, \tag{3}$$

where $\widehat{L} = \partial_z + c^{-1}d_t$ and α is the resonant absorption coefficient. By means of the Fourier transform,

$$F(\nu) = \int_{-\infty}^{+\infty} f(t)e^{i\nu(t-t_0)}dt. \tag{4}$$

Eqs. (2) and (3) are reduced to

$$\sigma_{eg}(z,\nu) = -\frac{\Omega(z,\nu)}{\nu + i\gamma}, \tag{5}$$

$$\left[\frac{\partial}{\partial z} - \frac{i\nu}{c} + A(\nu)\right] = 0, \tag{6}$$

where

$$A(\nu) = \frac{i\alpha\gamma/2}{\nu + i\gamma}. \tag{7}$$

The solution of Eq. (6) is

$$\Omega(z,\nu) = \Omega(0,\nu)\exp\left[(i\nu z/c) - A(\nu)z\right], \tag{8}$$

where $\Omega(0,\nu)$ is the Fourier transform of the input field envelope at the front face of the absorber with the coordinate $z = 0$. The inverse Fourier transform gives the familiar expression for the development of the radiation field in the resonant absorber with distance, that is

$$\Omega(z,t) = \frac{1}{2\pi}\int_{-\infty}^{+\infty}\Omega(0,\nu)\exp\left[-i\nu(t - z/c) - A(\nu)z\right]. \tag{9}$$

Below for simplicity of notations we disregard z/c in Eq. (9) since it is small for samples, used in gamma-optics. Actually, it is quite easy to incorporate this retardation parameter into final expressions [for example, in Eq. (10)] by simple substitution $t \to t - z/c$.

For the input field, given by Eq. (1) with $t_0 = 0$, the output field for the absorber of thickness z is (see Ref. [4, 9])

$$\Omega(z,t) = e^{-\gamma t}\Omega_0\Theta(t)J_0\left(2\sqrt{bt}\right), \tag{10}$$

where , Ω_0 is the maximum amplitude of the radiation field at the input ($z = 0$) if $t = 0$, $J_0(x)$ is the zero-order Bessel function, and $b = \alpha z\gamma/2 = \alpha z\Gamma/4$. According to Eq. (5) and solution (10), the spatiotemporal evolution of the matter coherence is given by the following explicit formula

$$\sigma_{eg}(z,t) = ie^{-\gamma t}\Omega_0\Theta(t)\int_0^t J_0\left(2\sqrt{b\tau}\right)d\tau, \tag{11}$$

which is derived with the help of the convolution theorem. The integration yields (see Ref. [11])

$$\sigma_{eg}(z,t) = ie^{-\gamma t}\Theta(t)\Omega_0 t\frac{J_1\left(2\sqrt{bt}\right)}{\sqrt{bt}}, \tag{12}$$

where $J_1(x)$ is the first-order Bessel function.

The coherence $\sigma_{eg}(z,t)$ is pure imaginary since the radiation field is in exact resonance. Depending on the sign of the function $J_1\left(2\sqrt{bt}\right)$ the phase of the coherence is $+\pi/2$ or $-\pi/2$ with respect to the phase of the incident field $\Omega_0\exp(-\gamma t)$. Since the argument of

this function, $2\sqrt{bt} = \sqrt{\alpha z \Gamma t}$, depends on time t and distance z, the sign of the phase shift of the matter coherence alternates with time and distance.

Spatial dependencies of the radiation field $\Omega(z,t)$ (dotted line) and imaginary part of the coherence $\sigma_{eg}(z,t)$ (solid line) along the sample at $\Gamma t = 1$ are shown in Fig. 1. It is clearly seen that in the domains I and III the imaginary part of the coherence is positive, while in the domain II it is negative. Thus, the absorber is divided into domains with alternating sign of the matter coherence or polarization. Therefore the scattered fields, re-emitted by different layers of the absorber, interfere with the incident field either destructively or constructively. This results in a fast damping of the leading edge of the output radiation pulse, followed by the dynamical beats, which may be viewed as a superposition of the incident field and scattered fields in different domains.

With time the sizes of the domains with the same phase of the polarization, i.e, the sizes of the homogeneous polarization layers, shorten inversely proportional to $\alpha\Gamma t$. These sizes can be expressed via cooperative length $L_c = c/\omega_c$ as the distances proportional to $L_c^2/(ct)$, where $\omega_c = (8\pi d_{eg} N\omega/\hbar)^{1/2}$ is the well-known cooperative frequency of the two-level medium and N is the density of resonant particles in it. For example, the absorber is completely covered by the domain I if the length of the absorber is $14.68 L_c^2/(ct)$ or $14.68/(\alpha\Gamma t)$. Since Γt is not to be large (otherwise the radiation field and polarization become exponentially small) the coherent effects, discussed in this paper, appear only in thick samples, i.e., if the condition $\alpha L_a > 14.68/\Gamma t$ is satisfied, where L_a is the absorber length. In terms of the cooperative frequency ω_c this condition demands that ω_c is to be larger or of the order of $4\sqrt{c\gamma/L_a}$. The latter condition is similar to the well-known condition for the existence of the oscillatory regime in superradiance [12] and implies relatively small incoherent decay rate γ, large cooperative frequency ω_c, and large sample length L_a.

III. ONE-SAMPLE ABSORBER

In this section we consider the absorber consisting of only one sample, see Fig. 2(a). If the sample is displaced instantaneously by the half-wavelength of the gamma-radiation, $\Delta z = \lambda/2$, along the direction of the field propagation, the phase of the coherence of each particle at the new locations, $z + \Delta z$, acquires an additional phase shift, $k\Delta z = \pi$, with respect to the phase of the incident plane wave $\propto \exp(-i\omega t + ikz)$, described by Eq. (1).

Therefore, the phase of the re-emitted, i.e, coherently scattered radiation (dipoles ringing) changes by π after the displacement. The displacement can be considered as an instantaneous if it takes place very fast with respect to all slow frequencies in the system, including γ and b.

We choose the moment of time $t_d > t_0$ of the instantaneous sample displacement, $\Delta z = \lambda/2$, when the coherence of the particles, located at the output of the sample, reaches its first zero. By that time only the domain I (see Fig. 1) of the matter coherence (polarization) is formed in the sample.

To find the transients, induced by the instantaneous displacement of the sample, we consider the incident radiation field $\Omega(0,t)$ as consisting of two pulses, i.e.,

$$\Omega(0,t) = \Omega_1(0,t) + \Omega_2(0,t), \tag{13}$$

where $\Omega_1(0,t) = \Omega_0 e^{-\gamma t}[\Theta(t) - \Theta(t-t_d)]$ is the first pulse with a finite duration t_d and $\Omega_2(0,t) = \Omega_0\Theta(t-t_d)e^{-\gamma t}$ is the second pulse, which is applied at time t_d.

The calculation of the integral in Eq. (9) for these pulses is essentially simplified with the help of the response function technique (i.e., with the help of the method of Green's function), see Refs. [5, 6, 8], where according to the convolution theorem this integral is reduced to

$$\Omega_n(z,t) = \int_{-\infty}^{+\infty} \Omega_n(0,t-\tau)R(z,\tau)d\tau. \tag{14}$$

Here $R(z,t)$ is the Green's function, which describes the output radiation from a sample of thickness z, if the input radiation is a very short pulse whose shape is given by the Dirac delta function, $\delta(t)$. For a resonant sample with a natural absorption linewidth, Γ, the same as the linewidth of the emission line of the source nucleus, the Green's function is

$$R(z,t) = \delta(t) - \Theta(t)e^{-\gamma t}\sqrt{\frac{b}{t}}J_1\left(2\sqrt{bt}\right). \tag{15}$$

Calculating the integral in Eq. (14) for the two pulses, $\Omega_1(0,t)$ and $\Omega_2(0,t)$, we find that

$$\Omega_1(z,t) = \Omega_0 e^{-\gamma t}\left[\Theta(t)J_0\left(2\sqrt{bt}\right) - \Theta(t-t_d)J_0\left(2\sqrt{b(t-t_d)}\right)\right], \tag{16}$$

$$\Omega_2(z,t) = \Omega_0 e^{-\gamma t}\Theta(t-t_d)J_0\left(2\sqrt{b(t-t_d)}\right). \tag{17}$$

Below we calculate the fields $\Omega_1(z,t)$ and $\Omega_2(z,t)$ at the place of the photo-detector with coordinate Z. For simplicity, one can consider Z as a distance from the source to the detector.

This distance does not change after the absorber displacement. Actually, the distance Z is present only in the exponential factor in the field amplitude, i.e., in $\Omega(Z,t)\exp(-i\omega t+ikZ)$, while the slowly varying amplitude of the field, $\Omega(Z,t)$, does not depend on Z, but depends only on the physical thickness of the absorber, L_a, specifying the thickness parameter $b = \alpha L_a\Gamma/4$ in Eqs. (16), (17).

Before the absorber displacement at time t_d the amplitude of the radiation field at the output of the absosber coincides with that given in Eq. (10). Just after the displacement the input field $\Omega_1(0,t)$ is switched off but the dipoles in the sample continue to ring producing the coherently scattering field, which is known as free induction decay (FID), see discussion of this point in Ref. [13], appendix B. However, since the position of the dipoles is changed by $\lambda/2$ at t_d, the phase of the scattered field at the place of the photo-detector changes by π with respect to the phase of the field $\Omega_1(Z,t)\exp(-i\omega t+ikZ)$ just before the displacement. Therefore, the scattered field or FID after t_d is $\Omega_{FID}(Z,t)\exp(-i\omega t+ikZ) = -\Omega_1(Z,t)\exp(-i\omega t+ikZ)$.

The second pulse, $\Omega_2(0,t)$, traveling through the absorber, transforms at the place of the photo-detector to $\Omega_2(Z,t)\exp(-i\omega t+ikZ)$ because this pulse interacts with the absorber being at rest just after its displacement. Therefore, after t_d the total output field at the place of the photo-detector is $\Omega(Z,t) = -\Omega_1(Z,t)+\Omega_2(Z,t)$, where the common exponential factor $\exp(-i\omega t+ikZ)$ is omitted for simplicity of notations. Combining these results in one expression we obtain

$$\Omega(Z,t) = \Omega_0 e^{-\gamma t}\Theta(t)\left\{[1-2\Theta(t-t_d)]\,J_0\left(2\sqrt{bt}\right)+2\Theta(t-t_d)J_0\left(2\sqrt{b(t-t_d)}\right)\right\}. \quad (18)$$

To some extent, this expression is similar to the expression for the so called "gamma-echo", produced by the instantaneous displacement of the radiation source with respect to the absorber being at rest, see Refs. [5, 6]. However, the phase of the field $\Omega(Z,t)\exp(-i\omega t+ikZ)$ in Eq. (18), which is produced by the sample displacement, is opposite to the phase of the gamma-echo at $t \geqslant t_d$ and coincides with the phase of the radiation field that would exist without the absorber displacement.

It is remarkable that the expression in curly brackets in Eq. (18) has absolute maximum value at $t = t_d$, which is $-J_0\left(2\sqrt{bt_d}\right)+2 = 2.403$, if at this time the matter coherence (polarization) at the output of the sample, L_a, is zero, $\sigma_{eg}(L_a,t_d) = 0$. This is because the first zero of the Bessel function of the first order, $J_1\left(2\sqrt{bt_d}\right) = 0$, takes place when the

zero-order Bessel function has its first negative extremum, $J_0\left(2\sqrt{bt_d}\right) = -0.403$, (see Fig. 1). This condition is satisfied if $bt_d = 3.67$.

For the first time the possibility to reach the absolute maximum in the transient signal of the gamma-echo for a particular value of the product bt_d was found by Helisto *et al.* in Ref. [5], however without mentioning of this phenomenon connection to the specific distribution of the matter coherence in the absorber. In Ref. [5] it was shown that the maximum probability (which is the amplitude squared) of the echo signal is 5.77 times larger than the probability of the resonant fraction of the input radiation just before t_d if $bt_d = 3.67$.

The radiation burst, induced by the sample displacement, is explained as follows. Before the moment of the displacement t_d the phase of the polarization in the domain I (see Fig. 1) is such that it is absorptive, since it generates the coherently scattered field, which is in antiphase with the incident radiation field. Therefore, the incident and scattered fields interfere destructively producing radiation damping. This is the basic mechanism of the attenuation of the field propagating through the absorber.

The shift of the polarization phase by π makes the resonant particles emissive since due to the phase shift the coherently scattered field becomes in phase with the incident radiation field and both fields interfere constructively. This is seen as the radiation burst at the output of the sample.

The instantaneous phase shift is actually an idealization. If the sample displacement is not instantaneous, then one has to take into account a continual character of the sample motion, which takes place during some finite time interval. This can be done by choosing the reference frame moving with sample. In this frame the sample, being at rest, experiences the input radiation field with the variable phase $\varphi(t) = k\delta z(t)$, where $\delta z(t)$ is the distance change between the source and the absorber. Calculating the output radiation from the absorber and performing the inverse transformation to the laboratory frame, we obtain

$$\Omega_\varphi(z,t) = \Omega_0\Theta(t)e^{-\gamma t}\left[1 - e^{i\varphi(t)}b\int_0^t e^{-i\varphi(t-\tau)}\frac{J_1\left(2\sqrt{b\tau}\right)}{\sqrt{b\tau}}d\tau\right]. \tag{19}$$

This expression can be transformed to (see Ref. [14])

$$\Omega_\varphi(z,t) = \Omega_0\Theta(t)e^{-\gamma t + i\varphi(t)}\left[e^{-i\varphi(0)}J_0\left(2\sqrt{bt}\right) + f_\varphi(t)\right], \tag{20}$$

where

$$f_\varphi(t) = -i\int_0^t \varphi_t'(t-\tau)e^{-i\varphi(t-\tau)}J_0\left(2\sqrt{b\tau}\right)d\tau. \tag{21}$$

Here $\varphi'_t(t-\tau)$ is a time derivative of the function $\varphi(t-\tau)$.

The influence of the phase-change rate, r, on the intensity of gamma-echo is analyzed in Ref. [8], where it is shown that the echo signal becomes recognizable if r is larger than the parameter b. Maximum intensity of the echo signal approaches to its ideal limit inherent for the instantaneous phase change if r is at least 10 times larger than b, see Ref. [14].

IV. TWO-SAMPLES ABSORBER: RADIATION BURST

In this section we consider two separate samples with thickness parameters $b_1 = \alpha L_1 \Gamma/4$ and $b_2 = \alpha L_2 \Gamma/4$, where L_1 and L_2 are their physical thicknesses. These samples are placed in a row along the propagation direction of the radiation field such that the first sample with the parameter b_1 interacts first with the source field, see Fig. 2(b).

The slowly varying amplitude, $\Omega(L_1,t)$, of the field at the output of the the first sample, $\Omega(L_1,t)\exp(-i\omega t + ikz_1)$, is described by Eq. (10), where b is to be substituted by b_1. In the exponential factor of the field, z_1 is a coordinate of the sample output. The input field for the second sample is $\Omega(L_1,t)\exp(-i\omega t + ikz_1 + ikd_{12})$, where d_{12} is a distance between the first and the second samples. With the help of Eq. (14) one can calculate the radiation field, $\Omega(z_2,t)\exp(-i\omega t + ikz_2)$, at the second-sample output (whose coordinate is z_2) and obtain the expression for the field amplitude, which is reduced to

$$\Omega(z_2,t) = \Theta(t)\Omega_0 e^{-\gamma t}\left[J_0\left(2\sqrt{b_1 t}\right) - \int_0^t J_0\left(2\sqrt{b_1(t-\tau)}\right)\sqrt{\frac{b_2}{\tau}}J_1\left(2\sqrt{b_2\tau)}\right)d\tau\right]. \quad (22)$$

The integral in Eq. (22) is calculated in the appendix A. The result, obtained there, allows to simplify the expression for $\Omega(z_2,t)$ to

$$\Omega(z_2,t) = \Theta(t)\Omega_0 e^{-\gamma t}J_0\left(2\sqrt{(b_1+b_2)t}\right). \quad (23)$$

This result is obvious since in the case of motionless samples their total effective thickness is just the sum of the effective thicknesses, b_1 and b_2, of the components constituting one effective sample with the length $L_1 + L_2$.

If the first sample experiences the instantaneous displacement by $\Delta z = \lambda/2$ and the second sample does not [see Fig. 2 (b)], then the amplitude, $\Omega(L_1,t)$, of the input field for the second sample, $\Omega(L_1,t)\exp(-i\omega t + ikz_{2in})$, is described by Eq. (18), where b is substituted by b_1. Here, by z_{2in} we denote the coordinate of the input face of the second

sample. The amplitude of the field at the output of the second sample with coordinate z_2 can be calculated with the help of Eq. (14). The result is

$$\Omega(z_2,t)=\Omega_0 e^{-\gamma t}\left\{\Theta(t)J_0\left(2\sqrt{(b_1+b_2)t}\right)+2\Theta(t-t_d)\left[F(t,t_d)-J_0\left(2\sqrt{b_1 t}\right)\right]\right\}, \quad (24)$$

where

$$F(t,t_d)=J_0\left(2\sqrt{(b_1+b_2)(t-t_d)}\right)+\int_0^{t-t_d}J_0\left(2\sqrt{b_1(t-\tau)}\right)\sqrt{\frac{b_2}{\tau}}J_0\left(2\sqrt{b_2\tau}\right)d\tau. \quad (25)$$

It is obvious that just after the displacement of the first sample the output field from the second sample demonstrates the spike whose maximum amplitude is

$$\Omega(z_2,t_d)=\Omega_0 e^{-\gamma t_d}\left[2-2J_0\left(2\sqrt{b_1 t_d}\right)+J_0\left(2\sqrt{(b_1+b_2)t_d}\right)\right]. \quad (26)$$

If time t_d and the effective thickness of the samples are chosen such that $b_1 t_d = 3.67$ and $b_2 t_d = 8.63$, then the coherence $\sigma_{eg}(z,t_d)$ is distributed along the first sample such that this sample is completely in the domain I (see Fig. 1). The distribution of the coherence $\sigma_{eg}(z,t_d)$ in the second sample corresponds to the case if the second sample is in the domain II (see Fig. 1). Fast displacement of the first sample makes its coherence emissive for the incident radiation field, $\Omega(0,t)$, since this field and the scattered field interfere constructively after the displacement. The coherence of the second sample is also emissive for the incident radiation field, $\Omega(0,t)$, since the field, scattered in this sample, interferes constructively with the incident field. As a result, we have a temporal amplification of the field in both absorbers instead of net absorption.

Thus, just before the displacement of the first sample ($t = t_d - 0$) its coherence, $-i\sigma_{eg}(z,t)$, is positive, and the coherence of the second sample, $-i\sigma_{eg}(z,t)$, is negative. Therefore, the polarizations of the first sample and the second sample re-emit in opposite phases. Fast displacement of the first sample makes both coherences negative at $t = t_d + 0$, i.e., they become both emissive and polarizations of the two samples emit the fields interfering constructively with the incident radiation field. To realize this case the second sample is to be 2.35 times thicker than the first sample.

With these parameters we have $2J_0\left(2\sqrt{b_1 t_d}\right) = -0.806$ and $J_0\left(2\sqrt{(b_1+b_2)t_d}\right) = 0.3$. Then the maximum amplitude of the spike is 3.1 times larger that the amplitude of the source radiation $\Omega_0 \exp(-\gamma t_d)$ just before the first-sample displacement, and the intensity is 9.6 time larger than the intensity of the input radiation at t_d. Comparison of the echo

signals from one and two samples is shown in Fig. 3, where the probability $P(t) = |a(z,t)|^2$ is plotted versus time t. For the plot Fig. 3(a) we take $\Gamma t_d = 1$, $b_1 = 3.67\Gamma$, and $b_2 = 8.63\Gamma$, and for Fig. 3(b) the parameters are $\Gamma t_d = 3$, $b_1 = 1.22\Gamma$, and $b_2 = 2.87\Gamma$. In the case of one sample we take $L_a = L_1$ and for two samples their total length is $L_{tot} = L_1 + L_2$. The distance between two samples is neglected. It is clearly seen from the plots that the signal from two samples is shorter and stronger than the signal from one sample. The echo intensity is smaller in Fig. 3(b) than in Fig. 3(a) because of the exponential factor, $\exp(-\gamma t_d)$, decreasing the amplitudes of the source radiation and coherently scattered fields by time t_d when the sample displacement is applied.

If the position of the first sample changes not instantaneously, then the amplitude of the input radiation field for the second sample is described by Eq. (19). Calculating the amplitude of the output radiation from the second sample, with the help of Eq. (14) we obtain

$$\Omega_\varphi(z_2,t) = \Theta(t)\Omega_0 e^{-\gamma t}\left[J_0\left(2\sqrt{b_2 t}\right) + F_1(b_1,t) + F_{12}(b_1,b_2,t)\right], \tag{27}$$

where

$$F_1(b_1,t) = -e^{i\varphi(t)} b_1 \int_0^t e^{-i\varphi(t-\tau)} \frac{J_1\left(2\sqrt{b_1\tau}\right)}{\sqrt{b_1\tau}} d\tau, \tag{28}$$

$$F_{12}(b_1,b_2,t) = b_1 b_2 \int_0^t d\tau_1 \int_0^{t-\tau_1} d\tau_2 e^{i\varphi(t-\tau_1)-i\varphi(t-\tau_1-\tau_2)} \frac{J_1\left(2\sqrt{b_2\tau_1}\right)}{\sqrt{b_2\tau_1}} \cdot \frac{J_1\left(2\sqrt{b_1\tau_2}\right)}{\sqrt{b_1\tau_2}}. \tag{29}$$

To estimate the influence of the time interval and the rate of the displacement on the amplitude and duration of the radiation spike we model the phase evolution by the function

$$\varphi(t) = \tan^{-1}[r(t-t_d)] + \pi/2. \tag{30}$$

It changes from 0 to π with the rate r. A time derivative of $\varphi(t)$, which is an instantaneous frequency of the radiation field in the reference frame moving with the first sample, is

$$\varphi_t'(t) = \frac{r}{1 + r^2(t-t_d)^2}. \tag{31}$$

Two examples of the transient-signal modification for different values of r are shown in Fig. 4. If $r = 10(b_1 + b_2)$ the echo signal almost reproduces the signal in ideal case of the instantaneous phase shift, except the sharp peak at the top, which is smoothened. If the rate r is only three times larger than $b_1 + b_2$, then the maximum intensity of the signal drops essentially. However, the echo signal is still recognizable.

V. TWO-SAMPLES ABSORBER: RADIATION QUENCHING

In this section we consider the case if only the second sample experiences the instantaneous displacement. If before the moment of time t_d of the displacement the first sample was in the domain I and the second sample was in the domain II, then, after t_d the sign of the second-sample coherence, $-i\sigma_{eg}(z,t)$, becomes positive, i.e., the same as the phase of the first-sample coherence. Therefore, the scattered fields in both samples will interfere destructively with the incident radiation field, $\Omega(0,t)$. Thus, due to the displacement the second sample becomes also absorptive and we expect the radiation quenching.

We calculate the output radiation field from the second sample as follows. The amplitude of the radiation field at the output of the first sample, $\Omega(z_1,t)$, is described by Eq. (10), where the parameter b is substituted by b_1. According to the arguments, given in the beginning of Sec. IV, the radiation field at the output of the second sample before t_d is described by Eq. (23).

To find the output field from the second sample after t_d we use the same approach as in Sec. III. We represent the input field for the second sample as consisting of two pulses, that is

$$\Omega(z_1,t) = \Omega_1(z_1,t) + \Omega_2(z_1,t). \tag{32}$$

where

$$\Omega_1(z_1,t) = [1-\Theta(t-t_d)]\Omega(z_1,t) \tag{33}$$

is a pulse with a duration t_d,

$$\Omega_2(z_1,t) = \Theta(t-t_d)\Omega(z_1,t) \tag{34}$$

is a pulse, which is applied at t_d, and $\Omega(z_1,t) = \Omega_0\Theta(t)J_0\left(2\sqrt{b_1 t}\right)\exp(-\gamma t)$.

The second pulse, $\Omega_2(z_1,t)$, interacts with the second sample only after its displacement. Therefore, according to Eq. (14), the output field for the second pulse is

$$\Omega_2(z_2,t) = \Theta(t-t_d)\Omega_0 e^{-\gamma t}\left[J_0\left(2\sqrt{b_1 t}\right) - G(t,t_d)\right], \tag{35}$$

where

$$G(t,t_d) = b_2\int_0^{t-t_d} J_0\left(2\sqrt{b_1(t-\tau)}\right)\frac{J_1\left(2\sqrt{b_2\tau}\right)}{\sqrt{b_2\tau}}d\tau. \tag{36}$$

If the second sample would not move at t_d, then after t_d the first pulse would produce FID (the dipoles ringing), seen at the output of the second sample as

$$\Omega_1(z_2,t)=\Omega_0 e^{-\gamma t}\left\{\Theta(t)J_0\left(2\sqrt{(b_1+b_2)t}\right)-\Theta(t-t_d)\left[J_0\left(2\sqrt{b_1 t}\right)-G(t,t_d)\right]\right\}. \quad (37)$$

However, because the second sample instantly changes its position by $\Delta z=\lambda/2$ at t_d the phase of FID changes by π, that is $\Omega_{FID}(z_2,t)=-\Omega_1(z_2,t)$. Thus, after t_d the output field from the second sample is $\Omega(z_2,t)=-\Omega_1(z_2,t)+\Omega_2(z_2,t)$, and before t_d it is described by Eq. (23). Combining these results in one formula we obtain

$$\Omega(z_2,t)=\Omega_0 e^{-\gamma t}\left\{\left[\Theta(t)-2\Theta(t-t_d)\right]J_0\left(2\sqrt{(b_1+b_2)t}\right)+2\Theta(t-t_d)A(t,t_d)\right\}, \quad (38)$$

where

$$A(t,t_d)=J_0\left(2\sqrt{b_1 t}\right)-G(t,t_d). \quad (39)$$

At $t=t_d+0$ the amplitude of the signal is

$$\Omega(z_2,t_d)=\Omega_0 e^{-\gamma t_d}\left[-J_0\left(2\sqrt{(b_1+b_2)t_d}\right)+2J_0\left(2\sqrt{b_1 t_d}\right)\right]. \quad (40)$$

If $b_1 t_d=3.67$ and $b_2 t_d=8.63$, then at $t=t_d$ the first sample is in the domain I and the second sample is in the domain II. In this case the functions in square brackets of Eq. (40) take values $-J_0\left(2\sqrt{(b_1+b_2)t_d}\right)=-0.3$ and $2J_0\left(2\sqrt{b_1 t_d}\right)=-0.806$. As a result the amplitude of the signal is $-1.106\Omega_0\exp(-\gamma t_d)$, whose absolute value is appreciably larger than the absolute value of the field amplitude just before t_d. Thus, instead of radiation quenching we see the radiation enhancement. This is because the phase of the output field from the first sample is π at t_d and the coherence $-i\sigma_{eg}(z,t)$ of the sample is also negative. Thus, just before t_d the second sample absorbs the field, which enters this sample. Fast displacement of the second sample makes it emissive with respect to the field entering this sample.

To make a displacement, which produces the absorption enhancement or the radiation quenching, we consider two samples, which satisfy the relations $-J_0\left(2\sqrt{(b_1+b_2)t_d}\right)=0.403$ and $2J_0\left(2\sqrt{b_1 t_d}\right)=-0.403$ at a particular time t_d. These relations are satisfied if $b_1 t_d=2$ and $b_2 t_d=1.67$. Figure 5 illustrates that case when the output intensity (probability) of the radiation field experiences quenching after fast displacement of the second sample.

If the second-sample displacement is slow and described by the function $\delta(r)$, then the output radiation field is given by the following expression

$$\Omega(z_2,t)=\Omega_0 e^{-\gamma t}\left[J_0\left(2\sqrt{b_1 t}\right)-G_\varphi(t,t_d)\right], \quad (41)$$

where

$$G_{\varphi}(t,t_d) = b_2 e^{i\varphi(t)} \int_0^t e^{-i\varphi(t-\tau)} J_0\left(2\sqrt{b_1(t-\tau)}\right) \frac{J_1\left(2\sqrt{b_2\tau}\right)}{\sqrt{b_2\tau}} d\tau, \tag{42}$$

and $\varphi(t) = k\delta(r)$. This result is obtained considering the input radiation field for the second sample, $\Omega(z_1,t)$, in the reference frame moving with this sample, where $\Omega(z_1,t)$ acquires the phase factor $\exp[-i\varphi(t)]$. Then, the inverse transformation of the output radiation from the second sample to the laboratory frame yields another phase factor $\exp[i\varphi(t)]$.

VI. THREE-SAMPLES ABSORBER: RADIATION BURST

In this section we consider the propagation of the radiation field through three samples, two of which (the first and the third) experience fast displacements at the moment of time t_d, see Fig. 2(c). If by this time the coherence $-i\sigma_{eg}(z,t)$ is positive along the first sample, negative along the second sample, and again positive along the third sample, then the first sample is in the domain I, the second sample is in the domain II, and the third sample is in the domain III, see Fig. 1(c). Simultaneous fast displacements of the first and third samples by $\Delta z = \lambda$ make the coherences of all three samples negative. Then, these samples (the sandwich) become emissive due to the constructive interference of the scattered and incident radiation fields and we expect the radiation burst with the strongly increased intensity.

To describe this effect we follow the calculation schemes represented in Secs. IV and V. According to Sec. IV the output radiation field from the second sample is described by Eq. (24). Formally this field consist of two components:

$$\Omega_1(z_2,t) = \Omega_0\Theta(t)e^{-\gamma t} J_0\left(2\sqrt{(b_1+b_2)t}\right), \tag{43}$$

which is switched on at $t=0$, and

$$\Omega_2(z_2,t) = 2\Omega_0\Theta(t-t_d)e^{-\gamma t}\left[F(t,t_d) - J_0\left(2\sqrt{b_1 t}\right)\right], \tag{44}$$

which is switched on at $t=t_d$, i.e., after the displacement.

For the input field $\Omega_2(z_2,t)$ the output field from the third sample is calculated with the help of Eq. (14).

For the input field $\Omega_1(z_2,t)$ the output field from the third sample before and after t_d is calculated in the same way as the field $\Omega(z_2,t)$ was calculated in Sec. V, see Eqs. (32),(38).

The result of these calculations is

$$\Omega(z_3,t)=\Omega_0 e^{-\gamma t}\left[\Theta(t)J_0\left(2\sqrt{(b_1+b_2+b_3)t}\right)+2\Theta(t-t_d)B(t)\right], \tag{45}$$

where

$$B(t)=B_1(t)+B_2(t)+B_3(t)+B_4(t)+B_5(t), \tag{46}$$

$$B_1(t)=J_0\left(2\sqrt{(b_1+b_2+b_3)(t-t_d)}\right), \tag{47}$$

$$B_2(t)=-J_0\left(2\sqrt{b_1 t}\right)+J_0\left(2\sqrt{(b_1+b_2)t}\right)-J_0\left(2\sqrt{(b_1+b_2+b_3)t}\right), \tag{48}$$

$$B_3(t)=\int_0^{t-t_d}J_0\left(2\sqrt{b_1(t-\tau)}\right)\left[\sqrt{\frac{b_2}{\tau}}J_1\left(2\sqrt{b_2\tau}\right)+\sqrt{\frac{b_3}{\tau}}J_1\left(2\sqrt{b_3\tau}\right)\right]d\tau, \tag{49}$$

$$B_4(t)=-\int_0^{t-t_d}J_0\left(2\sqrt{(b_1+b_2)(t-\tau)}\right)\sqrt{\frac{b_3}{\tau}}J_1\left(2\sqrt{b_3\tau}\right)d\tau, \tag{50}$$

$$B_5(t)=-\int_0^{t-t_d}d\tau_1\int_0^{t-t_d-\tau_1}d\tau_2 J_0\left(2\sqrt{b_1(t-\tau_1-\tau_2)}\right)\sqrt{\frac{b_2}{\tau_2}}J_1\left(2\sqrt{b_2\tau_2}\right)\sqrt{\frac{b_3}{\tau_1}}J_1\left(2\sqrt{b_3\tau_1}\right). \tag{51}$$

Just after t_d ($t=t_d+0$) the functions $B_3(t)$, $B_4(t)$, and $B_5(t)$ are zero. Therefore, the expression in the square brackets of Eq. (45) at $t=t_d$ takes value

$$2\left[1-J_0\left(2\sqrt{b_1 t_d}\right)+J_0\left(2\sqrt{(b_1+b_2)t_d}\right)\right]-J_0\left(2\sqrt{(b_1+b_2+b_3)t_d}\right). \tag{52}$$

If at $t=t_d$ the samples are located in the domains I, II, and III, as it is specified above, then $b_1 t_d=3.67$, $b_2 t_d=8.63$, and $b_3 t_d=13.57$. In this case the amplitude of the radiation field at the output of the third sample is $\Omega(z_3,t_d)=3.65\Omega_0\exp(-\gamma t_d)$ and its intensity is $|\Omega(z_3,t_d)|^2=13.6\Omega_0^2\exp(-\Gamma t_d)$.

Thus, due to the simultaneous displacement of two samples in the three-samples absorber the output intensity of the radiation field increases 13.6 times with respect to the intensity of the incident radiation field just before the displacement. The radiation intensities at the output of the three-samples absorber and at the output of the one-sample absorber with the parameter $b_1 t_d=3.67$ are compared in Fig. 6. It is clearly seen from the plots that in the case of three samples the intensity of the spike at t_d appreciably increases and duration of the spike substantially shortens with respect to the case of one sample.

VII. EXPERIMENT

Our experimental setup is described in a very detail in Refs. [7, 8]. As a single sample we take a piece of 25 μm thick, 3×5 mm stainless steel (SS) foil, which is glued on a polyvinylidene fluoride (PVDF) piezo polymer transducer (thickness 28 μm, model LDT0-28K, Measurement Specialties, Inc.). PVDF film is coupled to a plexiglas backing of $\sim$ 2 mm thickness with epoxy glue. The PVDF film was driven with a square wave pulse from Ortec Gate&Delay Generator (Model 416A) or Mini-Circuits Model ZPUL-21 Pulse Amplifier. They were triggered by the positive/negative output of the 122 keV channel constant fraction discriminator. The rise time of the driving pulse was about 18 nsec and 10 nsec for Gate&Delay Generator and Pulse Amplifier, respectively.

Two-samples sandwich was constructed from the single sample consisting of SS foil (SS1), coupled to the PVDF film and plexiglas backing, which was modified by coupling the second stainless steel foil (SS2) to the opposite side of the plexiglas backing. We had only one specimen of the stainless steel foil, which had natural abundance of ^{57}Fe (2.1%). We were unable to modify the physical thickness of the SS foil. Its estimated effective thickness is $T = \alpha z = 5.2$, where $z = 25$ μm. The corresponding parameters b for the samples, constituting the two-samples absorber, are $b_1 = b_2 = 1.3\Gamma$.

Thus, our two-samples sandwich was not optimally designed to observe the maximum enhancement of the radiation burst. First, to observe this maximum the ratio b_2/b_1 is to be 2.35 (we had $b_2/b_1 = 1$). Second, the maximum of the radiation burst is observed if the displacement is applied at time t_d, which satisfies the relation $b_1 t_d = 3.67$ at least for the first sample. Since the parameter b_1 for our SS1 sample is 1.3Γ, i.e., it is small, then to satisfy this relation we have to take $t_d = 400$ ns. By this time, both the incident and scattered fields experience appreciable exponential decay due to the factor $\exp(-\Gamma t_d)$.

There are also two experimental problems, reducing the effect, which are the finite time resolution of our experimental setup and the difficulty in creating the instantaneous displacement of the absorber. If the displacement of the samples would be instantaneous, then the maximum probability of the spike at t_d [without exponential factor $\exp(-\Gamma t_d)$] would be 5.77 for one sample (SS1), while for our two samples (SS1 and SS2) with equal thickness this probability is 7.7. Meanwhile, for two samples with optimal thickness ($b_1 t_d = 3.7$ and $b_2 t_d = 8.63$) the latter would be 9.6.

At first sight, two samples demonstrate more enhancement of the radiation burst with respect to one sample even in the case of not optimal choice of the parameters of the samples. This is because the contribution of the term $J_0\left(2\sqrt{b_1 t_d}\right)$ in Eq. (26) is doubled for the two samples and it is not doubled for one sample, see Eq. (18), while the contribution of the term $J_0\left(2\sqrt{(b_1+b_2)t_d}\right)$ is not very large in Eq. (26) if $b_1 = b_2$ and $b_1 t_d = 3.7$.

However, two experimental limitations spoil the picture. First, the time resolution of our setup is 9.1(5) ns. It was obtained by least-square-fitting the experimental lifetime spectra with the convolution of the theoretical decay curve and a Gaussian distribution originating from the time resolution function of our experimental setup. Since the spike, produced by two samples, is narrower than the spike from one sample, then the finite time resolution of our setup decreases the observable peak intensity of the signal from the sandwich (SS1+SS2) more than the peak intensity of the signal from one sample (SS1).

The second reason of the signal decrease is a finite time of the sample displacement. SS foil is quite heavy with respect to the light piezo-polymer film. Thus, even relatively sharp step voltage, applied to the transducer, induces quite smoothened step of the displacement. Figure 7 demonstrates time evolution of the experimentally measured voltage across conducting plates on the PVDF film, loaded by SS foil. If the displacement of the sample follows this voltage, then we can derive the function describing the phase change $\varphi(t)$. We approximated the voltage step by the function, shown by dots in Fig. 7, and derived $\varphi(t)$, which is

$$\varphi(t) = \varphi_0 \frac{\exp[r(t-t_d)]}{1+\exp[r(t-t_d)]}. \tag{53}$$

where $r = 16.7\Gamma$ and φ_0 is a maximum phase change at the end of the step-voltage. If $\varphi_0 = \pi$, the rate of the voltage step is relatively high since r is almost an order of magnitude larger than $b_1 + b_2 = 2.6\Gamma$ (see discussion at the end of Sec. IV).

Figure 8 demonstrates comparison of the theoretical transient signals, induced in our sandwich (solid line) and single sample (dotted line) by the instantaneous displacement (a), and by the displacement, described by Eq. (53), (b). In ideal case of the instantaneous displacement the sandwich produces slightly larger signal than one sample. In case of the slow phase change these signals have almost the same maxima and they slightly differ in the duration of the spike, which is shorter for the sandwich. Meanwhile, the signal from the sandwich is appreciably larger if it is compared with the single sample, which has the same effective thickness, i.e., the parameter b of the single sample is $b = 2b_1$ (see Fig. 8c).

If we would increase the voltage step, applied to the first sample (SS1), for example, two times, one can expect that φ_0 in Eq. (53) would also increase two times. Then, the effective rate of the phase change increases. If, for example, $\varphi_0 = 2\pi$, then $\varphi(t)$ reaches the value π, when the maximum of the spike takes place, two times faster. Such an increase of the voltage step should increase the intensity of the transient signal. Figure 9 shows a comparison of the echo signal from the sandwich and the single absorber of the same thickness for the instantaneous displacement (a) and for the slow displacement with $\varphi_0 = 2\pi$ (b). Appreciable increase of the echo signal for the sandwich is clearly seen.

Unfortunately we cannot make experiments with the single sample consisting of two SS foils with total thickness $z = 50$ μm because such a sample is too heavy for the PVDF film and it is hard to expect the sample displacement as fast as it could be for a single SS foil.

Therefore, we decided to measure and compare in our experiments the signals from the sandwich and single SS foil. We expected that the physics of the nuclear coherence manipulation, proposed in our paper, is correct if both samples would demonstrate the signals of nearly the same intensity but different in durations. We also decided to make experiment with sandwich in inverse scheme, as it is discussed in Sec. V. The absence of the appreciable echo signal should demonstrate that two samples (SS1 and SS2) are mechanically uncoupled, i.e., the displacement of SS2 is not transferred to SS1.

Our experimental results are shown in Fig. 10. The echo signal is appreciably sharper for the sandwich compared with the single SS foil. The absence of the echo signal if the radiation source is placed before the SS2 sample, which does not move, confirms that SS1 and SS2 are mechanically uncoupled. In this case (the inverse scheme) the mechanical displacement of the SS1 sample does not produce the radiation revival.

We plan in future to make samples, enriched with ^{57}Fe. These samples, being physically thin, could have an appreciable effective thickness T and large parameters b_1 and b_2, which could be adjustable in a process of sample fabrication.

Another choice for the proof-of-principle experiment is 93-keV Mössbauer resonance of ^{67}Zn. This resonance has two advantages. First, the wavelength of 93-keV radiation is much shorter than the wavelength of 14.4 keV radiation, resonant for ^{57}Fe, and hence a faster phase change is achieved at the same velocity of the mechanical displacement of the absorber. Second, the natural linewidth of 93-keV transition in ^{67}Zn is 12 kHz. Therefore, the time scale of all transients is nearly 100 times longer with respect to ^{57}Fe and hence fine

details of the transients in ^{67}Zn are detectable in principle with conventional detectors and electronics.

VIII. DISCUSSION

Radiative coupling and decoupling of nuclei in two samples by a piston-like modulation of the position of the first sample, Refs. [16, 17], or moving it with a trapezoidal displacement profile, Ref. [18], were studied in forward scattering of synchrotron radiation and the nuclear exciton echo was discovered. However, as indicated in Ref. [16], this echo has an essentially different nature compared with the gamma echo, Refs. [5, 6].

To compare our results with those, which were observed with synchrotron radiation, we considered the influence of the stepwise displacement of the first sample on the output radiation from the second sample.

We calculated the probability amplitude, $a(t)$, of the output radiation from the second sample if the first sample, irradiated by a synchrotron pulse at $t = 0$, experiences the instantaneous displacement by $\lambda/2$ at $t_d > 0$ (see appendix B). The result is

$$a(t) = \delta(t) - e^{-\gamma t}\left[\Theta(t)\sqrt{\frac{b_1+b_2}{t}}J_1\left(2\sqrt{(b_1+b_2)t}\right) - 2\Theta(t-t_d)C(t)\right], \qquad (54)$$

where

$$C(t) = \sqrt{\frac{b_1}{t}}J_1\left(2\sqrt{b_1 t}\right) - \int_0^{t-t_d}\sqrt{\frac{b_1}{t-\tau}}J_1\left(2\sqrt{b_1(t-\tau)}\right)\sqrt{\frac{b_2}{\tau}}J_1\left(2\sqrt{b_2\tau}\right)d\tau. \qquad (55)$$

At $t = t_d$ the amplitude of the spike is

$$a(t_d) = -e^{-\gamma t_d}\left[\sqrt{\frac{b_1+b_2}{t_d}}J_1\left(2\sqrt{(b_1+b_2)t_d}\right) - 2\sqrt{\frac{b_1}{t_d}}J_1\left(2\sqrt{b_1 t_d}\right)\right]. \qquad (56)$$

This amplitude cannot exceed the radiation amplitude, proportional to $b_1 + b_2$, which is observed just after the synchrotron pulse (at $t = +0$), when the function $J_1\left(2\sqrt{(b_1+b_2)t}\right)/\sqrt{(b_1+b_2)t}$ is close to 1. This is because the synchrotron pulse creates a phased collective state of nuclei in both absorbers with the same value of the coherence $\sigma_{eg}(t)$ for all nuclei in the samples at $t = +0$. Then, this phased collective state decays. Fast displacement of one of the samples is capable to reconstruct the coherent collective state only partially.

A single photon is incapable to create such a coherent state instantly. Nuclear coherence, as it is shown in Fig.1, needs time to be created by a single photon and this coherence is inhomogeneous along the samples, demonstrating oscillations with distance. We found conditions when the first sample displacement makes phasing of the coherence along both samples. This phasing is capable to reconstruct completely the radiation field for a short time.

IX. CONCLUSION

First, let us formulate the main results of the paper. We showed that a single gamma-photon propagating in an optically thick resonant absorber induces the polarization (quantified by the induced nuclear transition moments). The phase and amplitude of the polarization depends on time and propagation distance such that the absorber may be viewed as a sandwich of layers possessing polarizations with opposite phases. We propose to make a fast displacement of odd layers by a half wavelength of the radiation field. This displacement brings in phase the polarization of all layers, which results in-phasing of the scattered field in the layers with the incident radiation field. As a result the scattered fields and the incident field interfere constructively producing radiation burst at the output of the absorber. We found the condition when the displacement of the even layers of the sandwich produces radiation quenching at the output of the absorber due to the destructive interference of the incident and scattered fields. Experimental verification of the effects of the constructive and destructive interference of the incident and scattering radiation fields due to the polarization phasing is performed.

We believe that the control of a single photon radiation field by means of fast displacements of the elements of thick composite absorbers could find applications in quantum information processing and quantum computing.

In gamma domain this method can be used to detect extremely small displacements of the absorber with an accuracy of about 0.5 $\mathring{A}$. For example, this technique could be employed for the calibration of displacements of the tip of scanning tunneling microscopes.

X. ACKNOWLEDGEMENTS

This work was supported by National Science Foundation (Grant No. 0855668), Russian Foundation for Basic Research (Grant No. 12-02-00263-a), and Program of Presidium of RAS "Quantum physics of condensed matter".

XI. APPENDIX A

To calculate the integral

$$I(t) = \int_0^t J_0\left(2\sqrt{b_1(t-\tau)}\right)\sqrt{\frac{b_2}{\tau}}J_1\left(2\sqrt{b_2\tau}\right)d\tau, \tag{57}$$

we apply the Laplace transform

$$F(p) = \int_0^{+\infty} e^{-pt}f(t)dt, \tag{58}$$

to the function $I(t)$. It can be done in a following way. First, the Laplace transform of the zero-order Bessel function, $J_0\left(2\sqrt{b_1 t}\right)$, is (see Ref. [19])

$$\frac{1}{p}e^{-b_1/p}. \tag{59}$$

Second, for the function, $\sqrt{b_2/t}J_1\left(2\sqrt{b_2 t}\right) = -J_0\left(2\sqrt{b_2 t}\right)'_t$, one can apply the differentiation theorem and obtain the following Laplace transform

$$1 - e^{-b_2/p}. \tag{60}$$

Since the integral $I(t)$ is the convolution of these two functions, the Laplace transform of the integral is a product of the two Laplace transforms, Eq. (59) and Eq. (60) , that is

$$\frac{1}{p}e^{-b_1/p} - \frac{1}{p}e^{-(b_1+b_2)/p}. \tag{61}$$

The inverse Laplace transform of this function is easily calculated (see Ref. [19]), which gives

$$I(t) = J_0\left(2\sqrt{b_1 t}\right) - J_0\left(2\sqrt{(b_1+b_2)t}\right). \tag{62}$$

XII. APPENDIX B

The probability amplitude of the radiation field at the output of the first sample, irradiated by the synchrotron pulse at $t = 0$, is (see, for example, Ref. [17])

$$a_{s1}(t) = \delta(t) - \Theta(t)e^{-\gamma t}\sqrt{\frac{b_1}{t}}J_1\left(2\sqrt{b_1 t}\right). \tag{63}$$

According to Eq. (14), at the output of the second sample this radiation is transformed as follows

$$a_{s2}(t) = \delta(t) + a_1(t) + a_2(t) + a_{12}(t), \tag{64}$$

where

$$a_1(t) = -\Theta(t)e^{-\gamma t}\sqrt{\frac{b_1}{t}}J_1\left(2\sqrt{b_1 t}\right), \tag{65}$$

$$a_2(t) = -\Theta(t)e^{-\gamma t}\sqrt{\frac{b_2}{t}}J_1\left(2\sqrt{b_2 t}\right), \tag{66}$$

$$a_{12}(t) = \Theta(t)e^{-\gamma t}\int_0^t \sqrt{\frac{b_1}{t-\tau}}J_1\left(2\sqrt{b_1(t-\tau)}\right)\sqrt{\frac{b_2}{\tau}}J_1\left(2\sqrt{b_2\tau}\right)d\tau. \tag{67}$$

With the help of the method, described in the appendix A, the Laplace transform, $I(p)$, of the integral, $I(t)$, in Eq. (67) can be easily calculated. The result is

$$I(p) = \left(1 - e^{-b_1/p}\right)\left(1 - e^{-b_2/p}\right). \tag{68}$$

This expression can be transformed to

$$I(p) = \left(1 - e^{-b_1/p}\right) + \left(1 - e^{-b_2/p}\right) - \left[1 - e^{-(b_1+b_2)/p}\right], \tag{69}$$

whose inverse Laplace transform is

$$I(t) = \sqrt{\frac{b_1}{t}}J_1\left(2\sqrt{b_1 t}\right) + \sqrt{\frac{b_2}{t}}J_1\left(2\sqrt{b_2 t}\right) - \sqrt{\frac{b_1+b_2}{t}}J_1\left(2\sqrt{(b_1+b_2)t}\right). \tag{70}$$

With this result Eq. (64) is reduced to

$$a_{s2}(t) = \delta(t) - \Theta(t)e^{-\gamma t}\sqrt{\frac{b_1+b_2}{t}}J_1\left(2\sqrt{(b_1+b_2)t}\right). \tag{71}$$

If the first sample experiences the instantaneous displacement by $\lambda/2$ at $t_d > 0$, the probability amplitude of the radiation field at the output of this sample is

$$a_{s1}(t) = \delta(t) - \left[\Theta(t) - 2\Theta(t-t_d)\right]e^{-\gamma t}\sqrt{\frac{b_1}{t}}J_1\left(2\sqrt{b_1 t}\right). \tag{72}$$

With the help of Eq. (14) one can calculate the amplitude of the output radiation from the second sample if the input field is $a_{s1}(t)$. The result is given in Eq. (54).

If the first sample experiences a slow displacement, then the output radiation from this sample is

$$a_{s1\varphi}(t) = \delta(t) - \Theta(t) e^{-\gamma t - i\varphi(t)} \sqrt{\frac{b_1}{t}} J_1\left(2\sqrt{b_1 t}\right), \tag{73}$$

where $\varphi(t) = k\delta r(t)$, see Sec. III. In this case the amplitude of the output radiation from the second sample is modified as follows

$$a_{s2\varphi}(t) = \delta(t) + a_{1\varphi}(t) + a_2(t) + a_{12\varphi}(t), \tag{74}$$

where

$$a_{1\varphi}(t) = -\Theta(t) e^{-\gamma t - i\varphi(t)} \sqrt{\frac{b_1}{t}} J_1\left(2\sqrt{b_1 t}\right), \tag{75}$$

$$a_{12\varphi}(t) = \Theta(t) e^{-\gamma t} \int_0^t e^{-i\varphi(t-\tau)} \sqrt{\frac{b_1}{t-\tau}} J_1\left(2\sqrt{b_1(t-\tau)}\right) \sqrt{\frac{b_2}{\tau}} J_1\left(2\sqrt{b_2\tau}\right) d\tau. \tag{76}$$

This expression is consistent with Eq. (3) in Ref. [18]. We compared numerically the intensities of the radiation fields $a(t)$ for the instantaneous displacement, Eq. (54), and $a_{s2\varphi}(t)$ for the slow displacement, Eq. (74), where $\varphi(t)$, Eq. (30), with $r \gg b_1 + b_2$ were used. Both functions coincide quite well if $r = 100(b_1 + b_2)$.

---

[1] A. Einstein, Ann. Phys. (Leipzig) **322**, 132 (1905).

[2] K. Hammerer, A. S. Sorensen, and E. S. Polzik, Rev. Mod. Phys. **82**, 1041 (2010).

[3] P. Kolchin, C. Belthangady, S. Du, G. Y. Yin, and S. E. Harris, Phys. Rev. Lett. **101**, 103601 (2008).

[4] F. J. Lynch, R. E. Holland, and M. Hamermesh, Phys. Rev. **120**, 513 (1960).

[5] P. Helisto, I. Tittonen, M. Lippmaa, and T. Katila, Phys. Rev. Lett. **66**, 2037 (1991).

[6] I. Tittonen, M. Lippmaa, P. Helisto, and T. Katila, Phys. Rev. B **47**, 7840 (1993).

[7] R. N. Shakhmuratov, F. Vagizov, J. Odeurs, and O. Kocharovskaya, Phys. Rev. A **80**, 063805 (2009).

[8] R. N. Shakhmuratov, F. Vagizov, and O. Kocharovskaya, Phys. Rev. A **84**, 043820 (2011).

[9] S. M. Harris, Phys. Rev. **124**, 1178 (1961).

[10] U. van Bürck, Hyperfine Interactions **123/124**, 483 (1999).

[11] I. S. Gradshteyn and I. M. Ryzhik *Table of Integrals, Series, and Products*, edited by A. Jeffrey and D. Zwillinger, (Academic Press, 2007).

[12] V.V. Zheleznyakov, V.V. Kocharovsky, Vl.V. Kocharovsky, Sov. Phys. Uspekhi **32**, 835 (1989).

[13] R. N. Shakhmuratov, Phys. Rev. A **85**, 023827 (2012).

[14] R. N. Shakhmuratov, F. Vagizov, and O. Kocharovskaya, Bulletin of the Russian Academy of Sciences. Physics **76**, 248 (2012).

[15] J. Ball and S.J. Lyle, Nucl. Instrum. Methods **163**, 177 (1979).

[16] G. V. Smirnov, U. van Bürck, J. Arthur, S. L. Popov, A. Q. R. Baron, A. I. Chumakov, S. L. Ruby, W. Potzel, and G. S. Brown, Phys. Rev. Lett. **77**, 183 (1996).

[17] G. V. Smirnov and W. Potzel, Hyperfine Interactions **123/124**, 633 (1999).

[18] P. Schindelmann, U. van Bürck, W. Potzel, G. V. Smirnov, S. L. Popov, E. Gerdau, Yu. V. Shvydko, J. Jäschke, H. D. Rüter, A. I. Chumakov, and R. Rüffer, Phys. Rev. A **65**, 023804 (2002).

[19] M. Abramowitz and I. A. Stegun, *Handbook of Mathematical Functions* (Dover, New York, 1965).

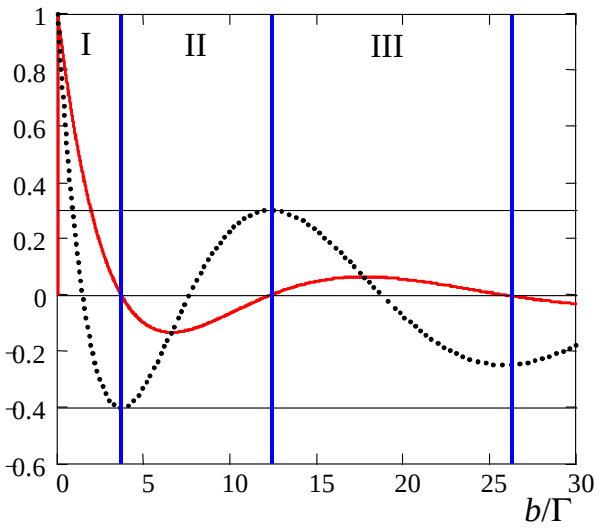

FIG. 1: (color on line) Spatial dependence of the propagating field (dotted black line) and the imaginary part of the matter coherence (polarization), multiplied by decay rate Γ, (solid line in red) in the absorbing medium at the moment of time satisfying the condition $\Gamma t = 1$. Parameter b is proportional to the distance z, counted along the propagation direction of the field from the front face of the absorber ($z = 0$). Both graphs are plotted without exponential factor $\exp(-\gamma t)$ and they are normalized to the input field amplitude Ω_0. Vertical bold blue lines divide the plot into domains (I, II, and III), where the imaginary part of the matter coherence (polarization) has the same sign (plus or minus). Thin horizontal lines show the values of the two first extrema of the radiation field amplitude.

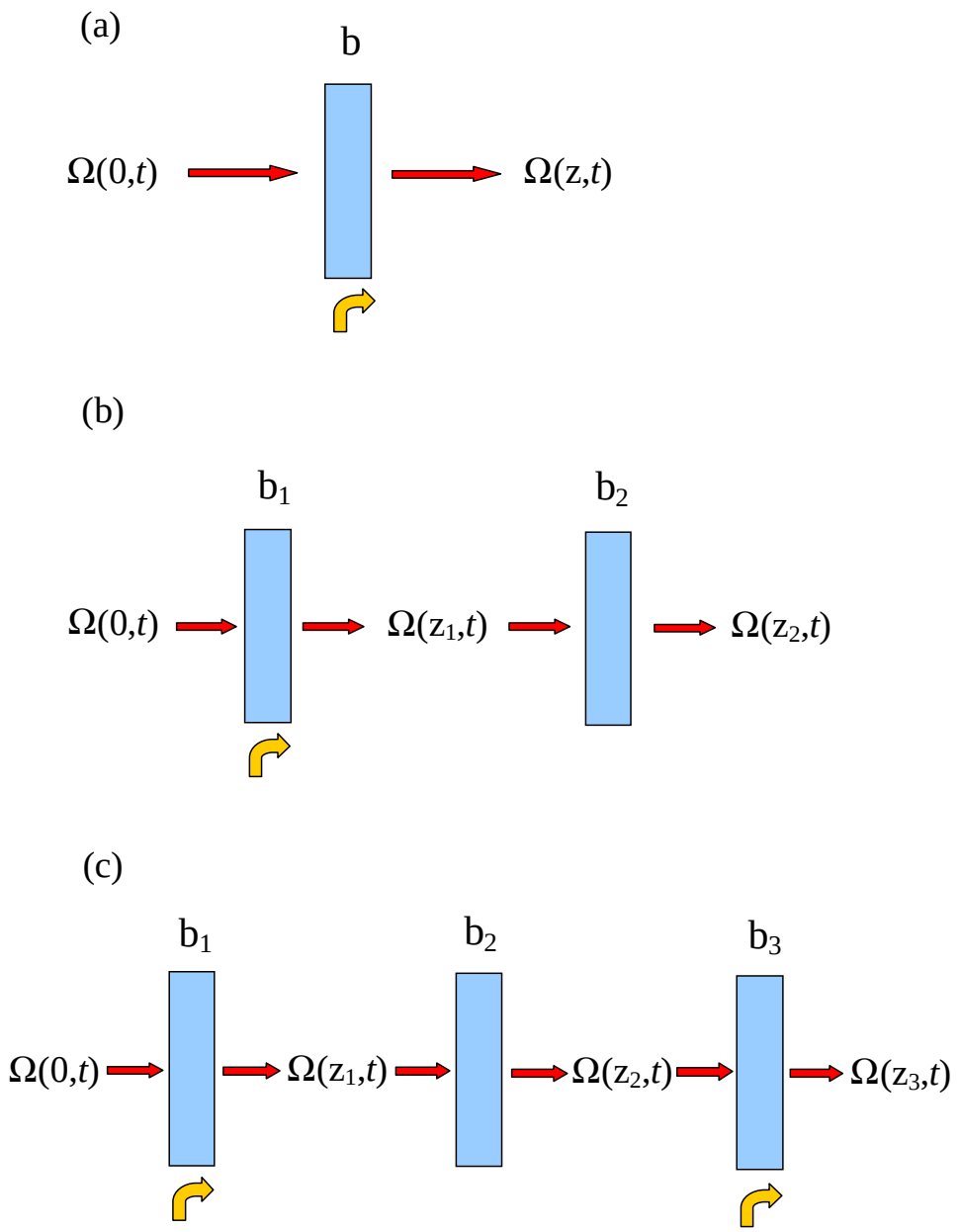

FIG. 2: (color on line) The excitation scheme for the sandwich absorber made of one (a), two (b), and three samples (c). The input and output radiation fields for each sample are shown by the straight arrows. The mechanical displacements, applied to a particular sample, are shown by the bent arrows. $\Omega(0,t)$ is the amplitude of the radiation field from the source. $\Omega(z_i,t)$ is the output radiation field from the i-th sample. Other notations are defined in the text.

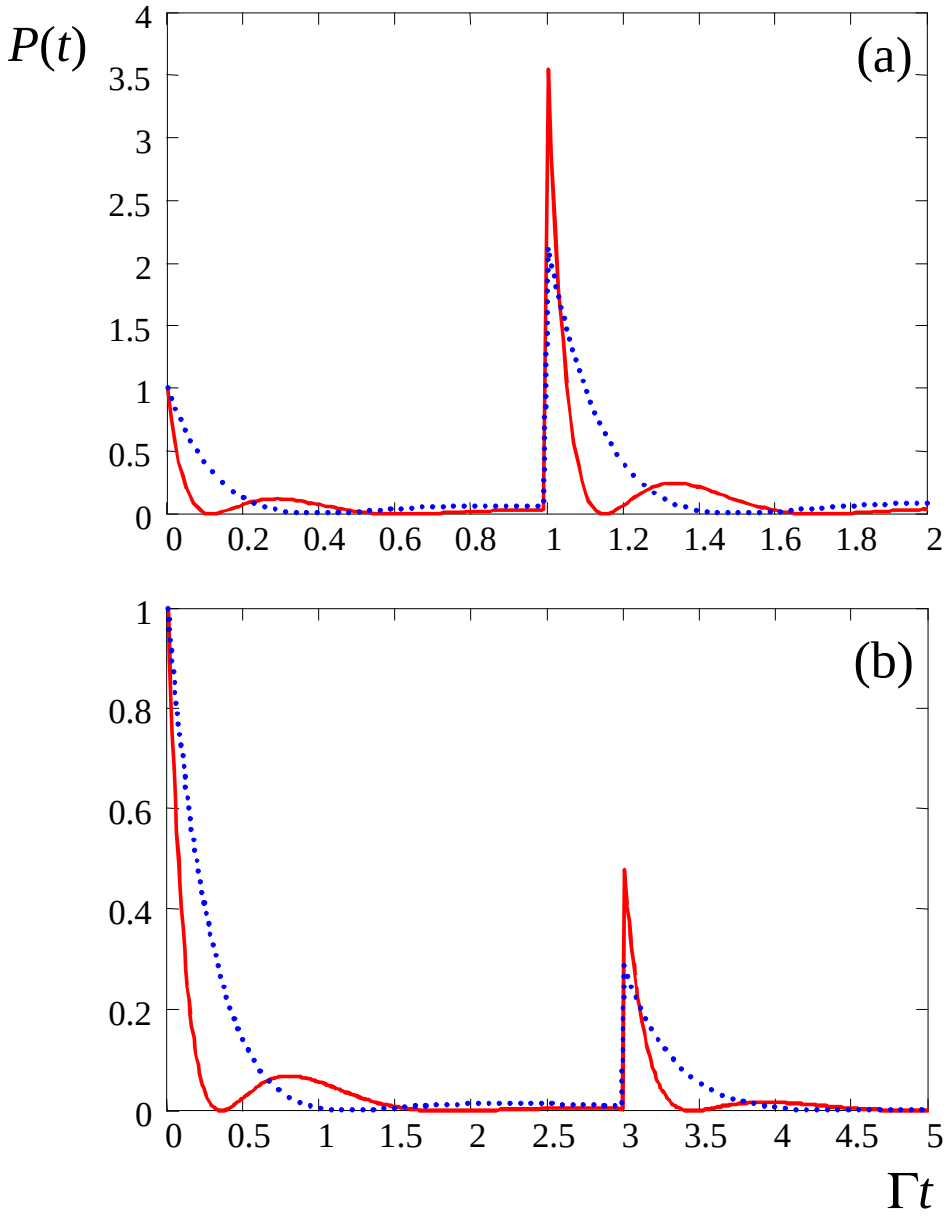

FIG. 3: (color on line) Comparison of time dependencies of the photon probabilities $P(t)$ (amplitude squared) at the output of one sample experiencing the instantaneous displacement (dotted line in blue) and at the output of two samples if only the first of the two samples experiences the instantaneous displacement (solid line in red). The parameters are $\Gamma t_d = 1$, $b_1 = 3.67\Gamma$, and $b_2 = 8.63\Gamma$ for plots (a) and $\Gamma t_d = 3$, $b_1 = 1.22\Gamma$, and $b_2 = 2.87\Gamma$ for plots (b). The probability of the input radiation field is normalized to 1.

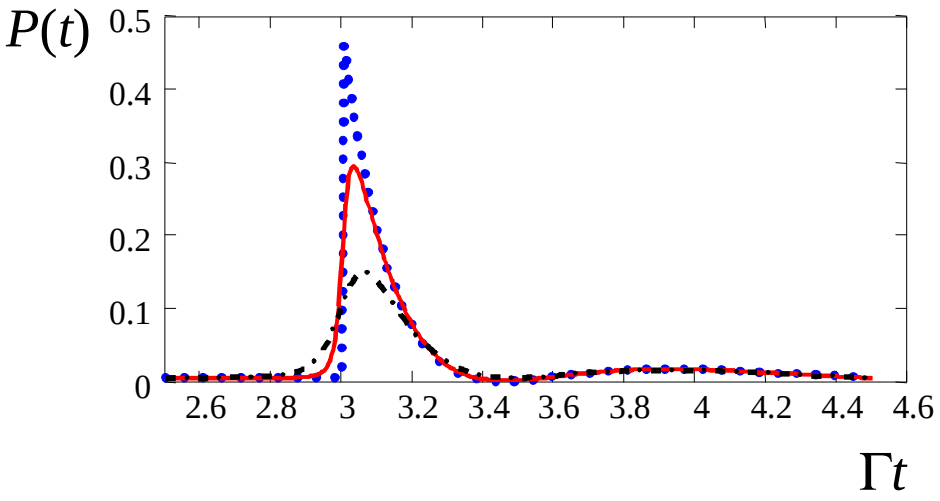

FIG. 4: (color on line) Time evolution of the detection probability $P(t)$ of the radiation at the output of the two-samples absorber with the parameters $b_1 = 1.22\Gamma$ and $b_2 = 2.87\Gamma$. Only zoom-in of the domain, where the echo signal takes place, is shown. The signal, induced by the instantaneous displacement of the first sample, is shown by dots (in blue). The red solid line shows the signal induced by the slow change of the sample position if the change rate is $r = 10(b_1 + b_2)$. The black dash-dotted line shows the signal for even slower rate of the displacement $r = 3(b_1 + b_2)$.

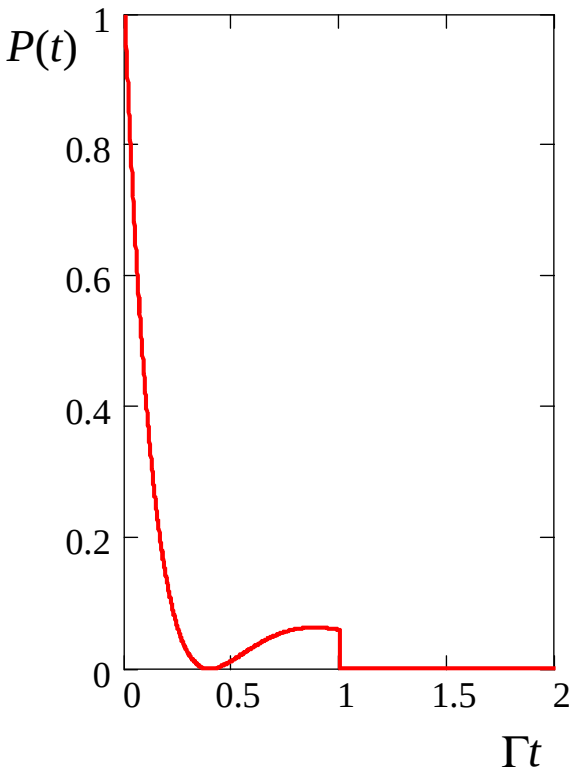

FIG. 5: (color on line) Time evolution of the detection probability $P(t)$ of the radiation at the output of the two-samples absorber with the parameters $b_1 = 2\Gamma$ and $b_2 = 1.67\Gamma$. The instantaneous displacement of the second sample, applied at $t_d = 1/\Gamma$, results in the abrupt quenching of the output radiation.

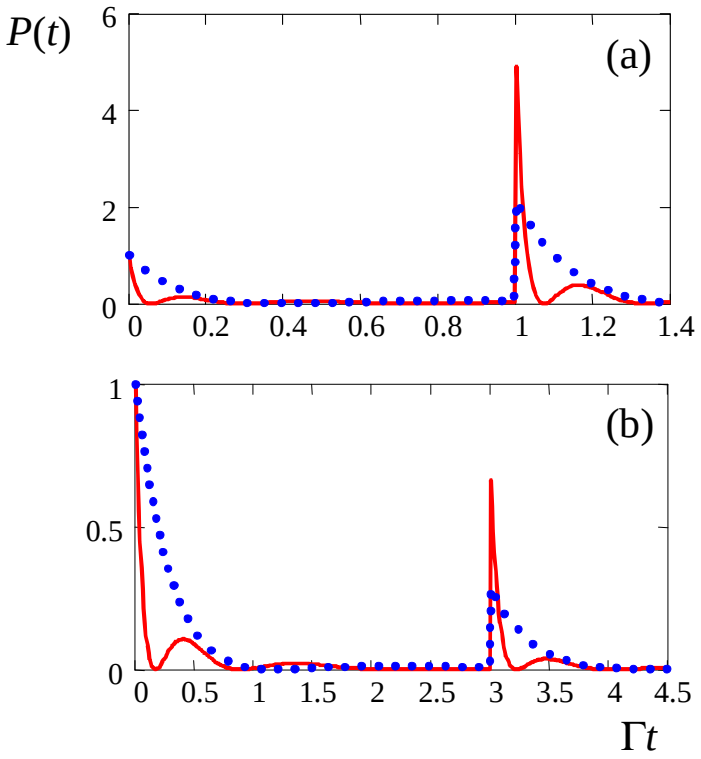

FIG. 6: (color on line) Time evolution of the detection probability $P(t)$ of the radiation at the output of the three-samples absorber with the parameters $b_1 t_d = 3.67\Gamma$, $b_2 t_d = 8.63\Gamma$, and $b_3 t_d = 13.57\Gamma$ (red solid line). The detection probability $P(t)$ of the radiation at the output of the one-sample absorber with the parameter $b_1 t_d = 3.67\Gamma$ is shown by (blue) dots for comparison. Time of the instantaneous displacement of the samples is $t_d = 1/\Gamma$ in (a) and $t_d = 3/\Gamma$ in (b).

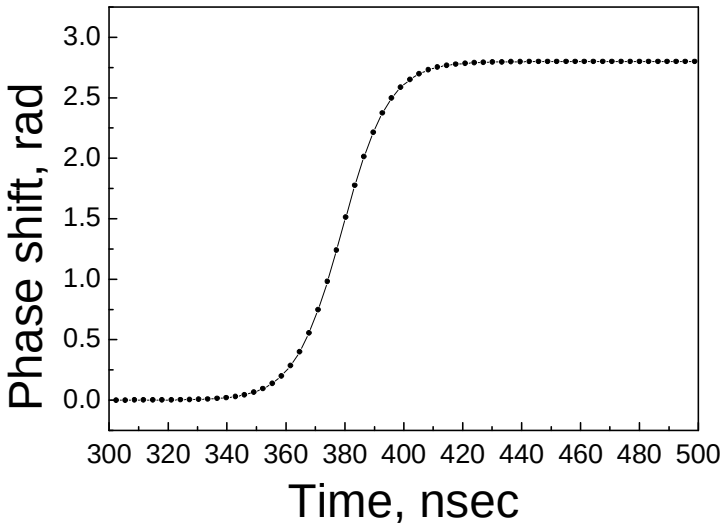

FIG. 7: Time evoltion of the experimentally measured voltage between conducting plates of PVDF film with the SS foil, glued on the top by epoxy, (solid line). Theoretical fitting of the experimental curve to Eq. (53) is shown by dots.

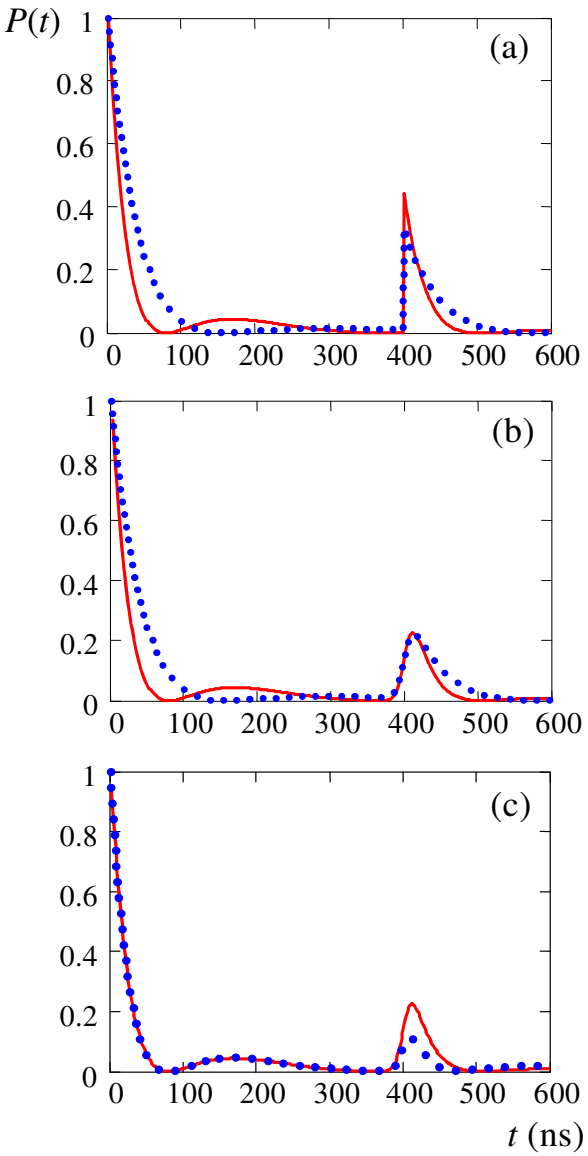

FIG. 8: (color on line) Time evolution of the detection probability of the radiation field at the output of the two-samples-sandwich absorber (red solid line) and one-sample absorber (blue dots) for the instantaneous phase shift (a) and for the slow displacement of SS1 (b). (c) Comparison of the detection probability for the two-samples-sandwich absorber (red solid line) and one-sample absorber of doubled thickness, if both foils (SS1 and SS2) would experience slow displacement together (blue dots).

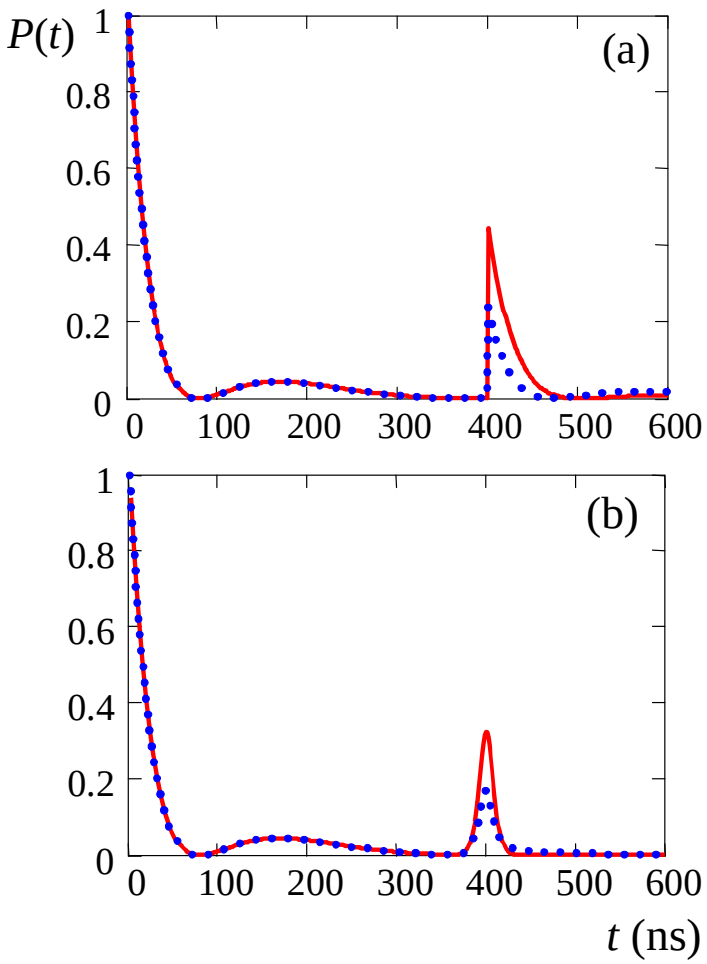

FIG. 9: (color on line) Time evolution of the detection probability of the radiation field at the output of the two-samples-sandwich absorber (red solid line) and one-sample absorber of the same thickness (blue dots) for the instantaneous phase shift (a) and for the slow displacement if $\varphi_0 = 2\pi$ (b).

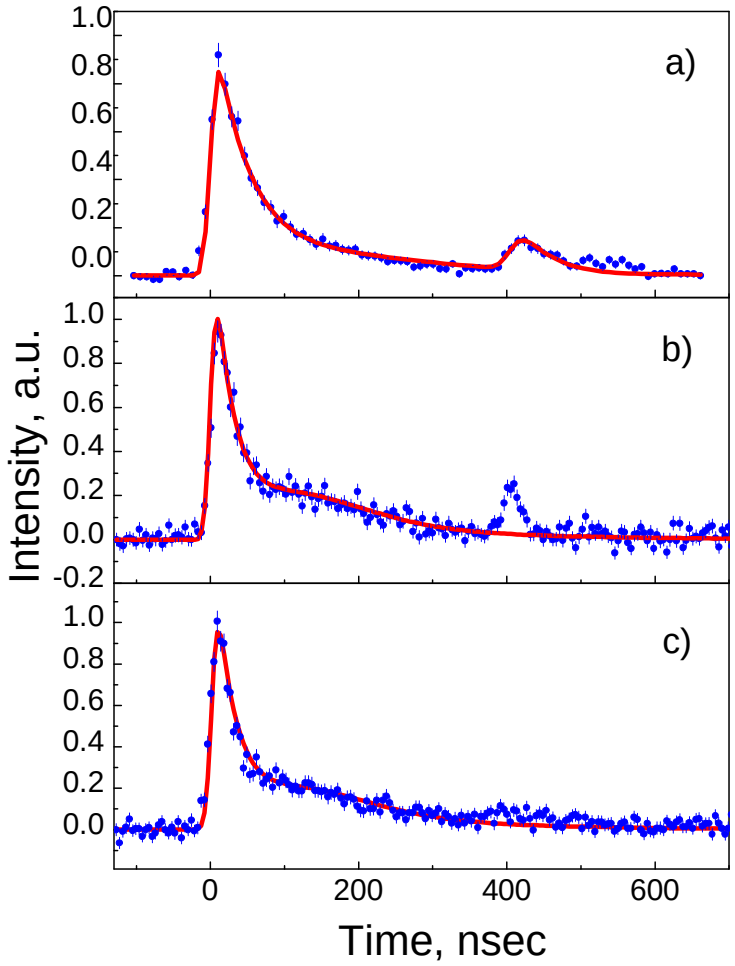

FIG. 10: (color on line) Output radiation intensity versus time. Mechanical displacement of the single sample (a), first sample (SS1) in the sandwich (b), and second sample (SS2) in the sandwich (c) is produced at 400 nsec after the detection of 122 keV photon. Dots (in blue) are experimental data. Solid line (in red) is a theoretical fit in (a) and a theoretical fit of the signal from the sandwich if the samples do not move in (b) and (c). The procedure of our theoretical fit, taking into account nonresonant fraction of the radiation field with recoil, is described in detail in Ref. [8].